

Supplementary Materials for

Structure of a Light-Activated LOV Protein Dimer That Regulates Transcription

Anand T. Vaidya, Chen-Hui Chen, Jay C. Dunlap, Jennifer J. Loros, Brian R. Crane*

*To whom correspondence should be addressed. E-mail: bc69@cornell.edu

Published 2 August 2011, *Sci. Signal.* **4**, ra50 (2011)
DOI: 10.1126/scisignal.2001945

The PDF file includes:

- Fig. S1. VVD-II has a high redox potential.
- Fig. S2. Comparison of the LSD structure of VVD with time-resolved SAXS data.
- Fig. S3. Targeting the cross-linking ability of the LSD of VVD.
- Fig. S4. The *csr-1* knock-in strains used in this study were homokaryons.
- Fig. S5. Light-dependent induction of *vvd* expression and VVD protein production in strains with various *vvd* mutant alleles.
- Fig. S6. Sequence similarity between VVD and WC-1.
- Fig. S7. Comparison of the light-induced changes in hydrogen bonding found for VVD and the *A. sativa* phototropin LOV2 domain.
- Table S1. Data collection and phasing statistics.
- Table S2. Conservation of light-dependent signaling and dimerization in the fungal LOV domains.
- Reference

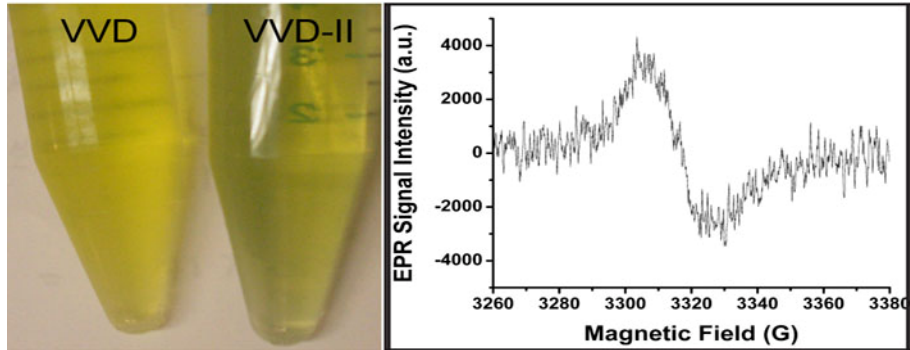


Fig. S1. VVD-II has a high redox potential. VVD-II was purified from *E. coli* in a partial neutral semiquinone state, which was indicated by the green color of the protein compared to the yellow color of the native protein (left panel) and the electron spin resonance (ESR) spectrum of VVD-II as measured with a 9-GHz cw ESR spectrometer (right panel).

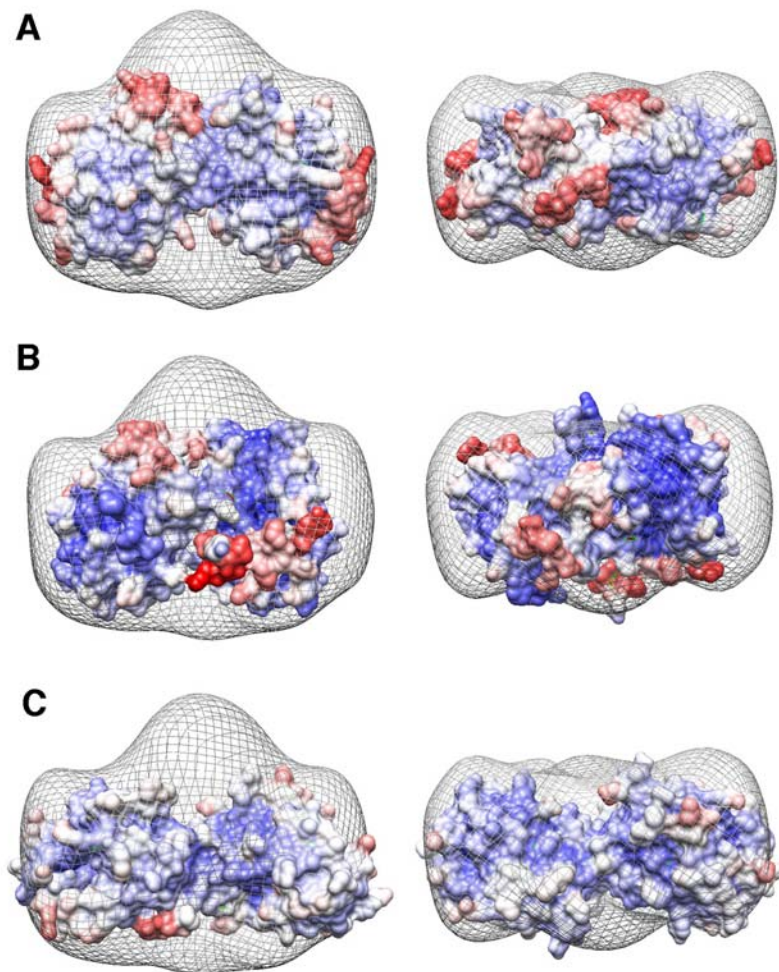


Fig. S2. Comparison of the LSD structure of VVD with time-resolved SAXS data. Superposition of the molecular envelope determined from time-resolved SAXS of light-state VVD and the solvent-accessible surface of several crystallographic dimers of VVD colored by relative thermal B-factor (blue, low; red, high). The views on the right are down from the top as shown on the left. The dimensions of the SAXS envelope generally matched those of the LSD of VVD (A), with the exception of a protrusion of SAXS density along the two-fold axis of the dimer; however, this small discrepancy likely reflected dynamics in this part of the molecule. Extended, mobile regions of the VVD structure (denoted by the red surface) pointed toward the two-fold axis of the dimer at the top of the envelope. Note that there is some ambiguity in fitting the structure within the envelope. The procedure that was used to calculate the SAXS envelope (*I*) does not account for conformational heterogeneity; rather, it assumes a constant protein density and a sharp boundary between solvent and protein, which in the more mobile regions of the protein is not a fully representative model. Other crystallographically characterized VVD dimers do not fit the SAXS envelope nearly as well as does the LDS structure. (B) The alternative non-physiological dimer present in the LSD crystal lattice. (C) The VVD dimer found in dark-state crystals (PDB Code: 2PD7).

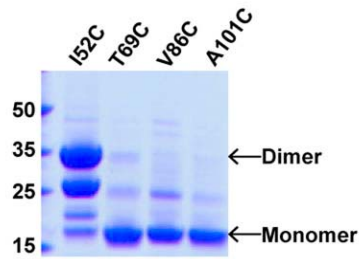


Fig. S3. Targeting the cross-linking ability of the LSD of VVD. The Ile⁵²→Cys variant VVD protein spontaneously cross-linked in the light when purified from *E. coli*, whereas variant proteins from which other positions from the dimer interface (Val⁸⁶ and Ala¹⁰¹) were removed did not cross-link. The band at 25 kD corresponds to proteolytically degraded dimeric VVD. The Thr⁶⁹→Cys substitution also placed a thiol at the dimer interface, but subunits of this variant protein did not cross-link readily, which may have been a result of the non-ideal orientation of the cysteine thiols to form disulfide bonds.

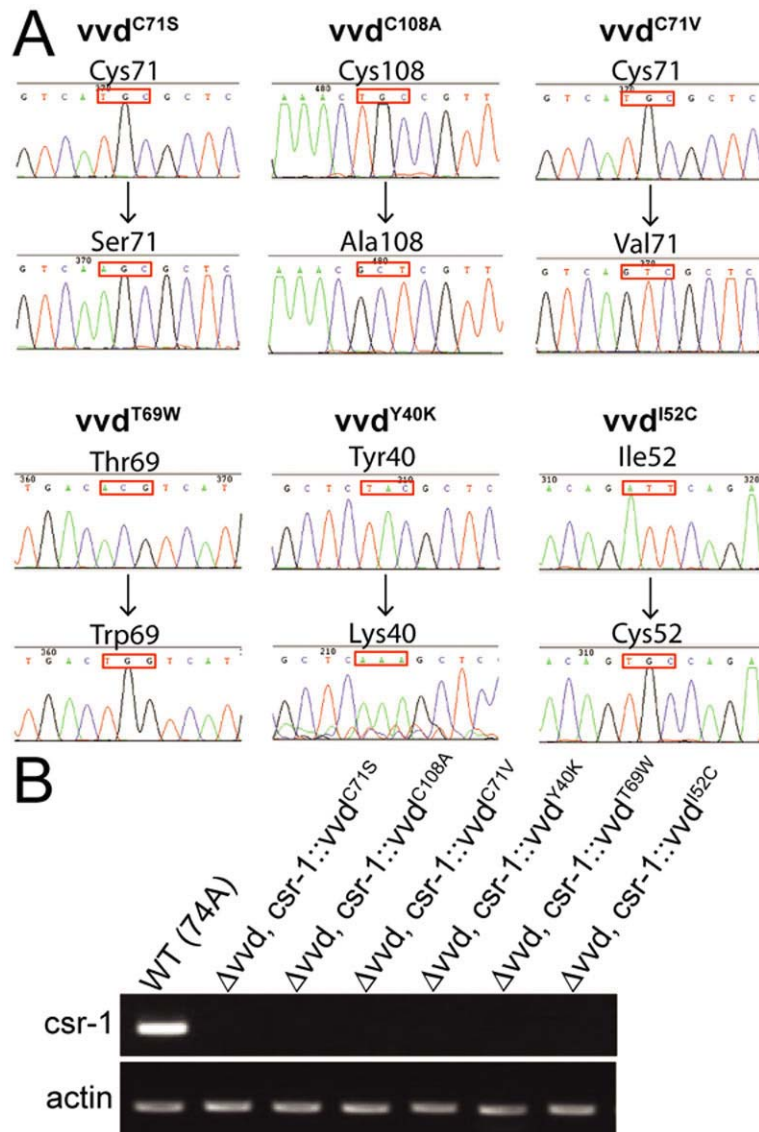


Fig. S4. The *csr-1* knock-in strains used in this study were homokaryons. **(A)** Sequencing data of various *vvd* mutant alleles. **(B)** PCR analysis of the absence of the *csr-1* locus in the genomes of each knock-in strain.

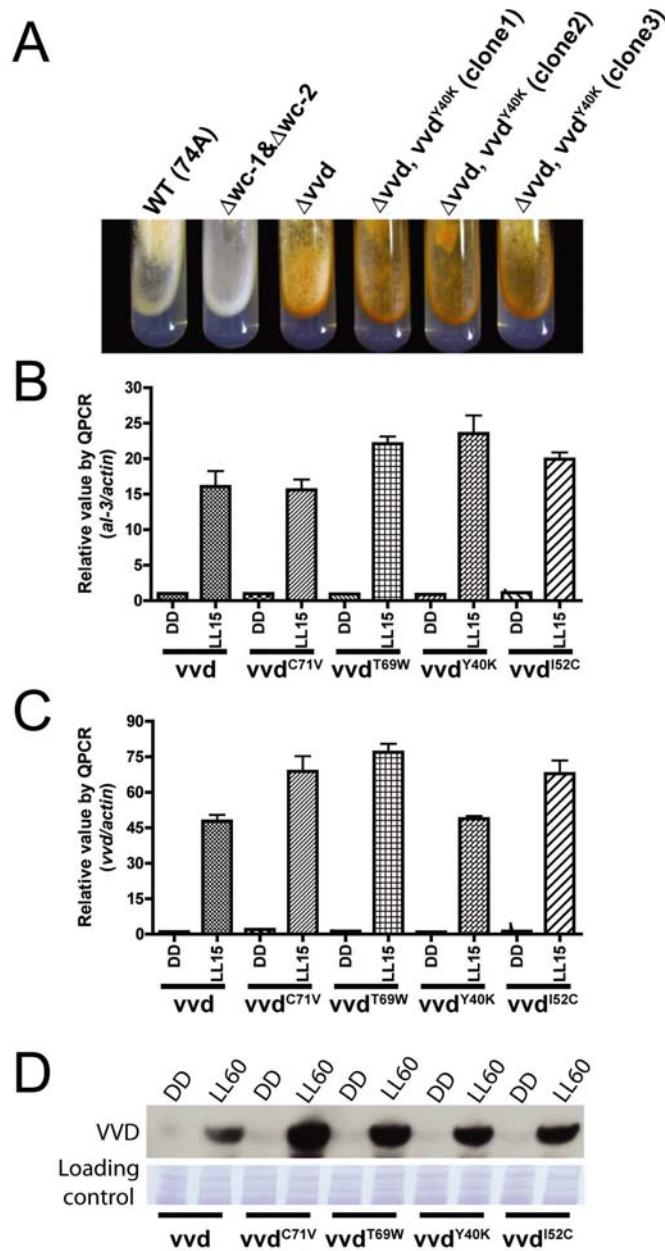


Fig. S5. Light-dependent induction of *vvd* expression and VVD protein production in strains with various *vvd* mutant alleles. **(A)** Independent primary transformants of *vvd*^{Y40K} mutant allele (clones 1, 2, and 3) displayed a consistent phenotype of photoadaptation defects. **(B)** Light-dependent induction of *al-3* and **(C)** *vvd* expression at LL15 in strains with various *vvd* mutant alleles was determined by RT-PCR analysis (n = 3 experiments). Data shown are mean values \pm standard errors. **(D)** Light-dependent induction of the production of VVD protein at LL60 in strains with various *vvd* mutant alleles. Upper panel shows Western blotting analysis of VVD tagged with a C-terminal V5 epitope with an antibody against V5. The lower panel shows the Coomassie-stained loading control.

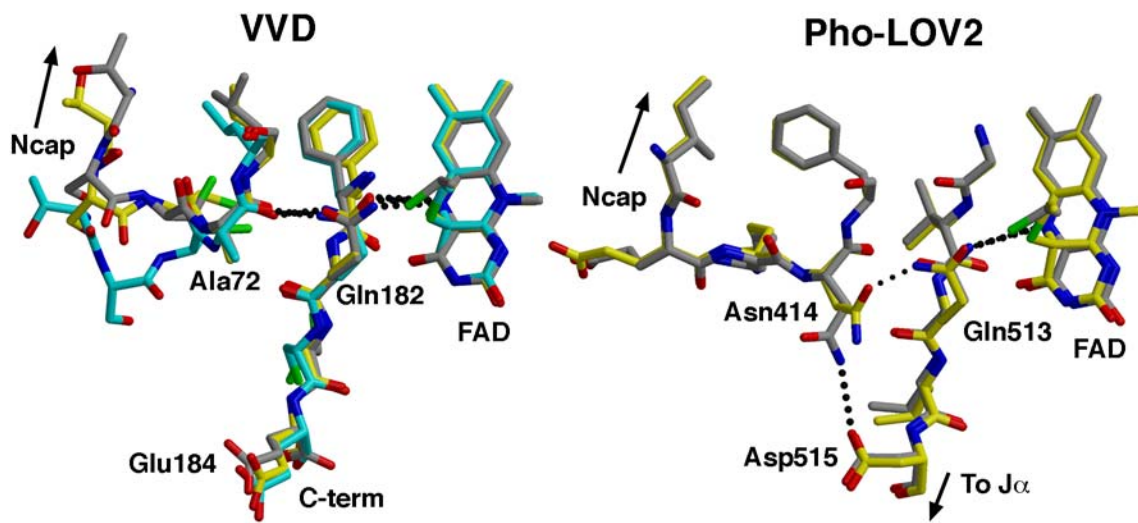


Fig. S7. Comparison of the light-induced changes in hydrogen bonding found for VVD and the *A. sativa* phototropin LOV2 domain. In both VVD (left panel) and the *A. sativa* phototropin LOV2 domain (right panel), formation of cysteinyl-flavin adducts caused similar changes to hydrogen bonding between the first and last β -strands of their respective PAS domains. In VVD, protonation of the N5 of flavin flipped Gln¹⁸² in the light state (yellow and cyan for the two superimposed subunits), which resulted in the formation of a new hydrogen bond to the carbonyl group of Ala⁷². In LOV2, the analogous glutamine residue formed a similar hydrogen bond with the first residue of the first β -strand in the light state (yellow), but in this case, the acceptor was the side chain of Asn⁴¹⁴, which no longer formed hydrogen bonds with Asp⁵¹⁵, as it does in the dark state (gray). In the VVD LSD, these changes resulted in restructuring of the linker loop leading to the N-cap. The changes in the cyan subunit were larger than those in the yellow subunit. No such large-scale changes were seen in the LOV2 Ncap; however, potential rearrangements were probably limited by the crystal lattice. *A. sativa* LOV2 domains are shown for PDB codes 2V1A (dark state) and 2V1B (light state).

Table S1. Data collection and phasing statistics. Data for outermost resolution shell are given in parenthesis.

<i>Parameter</i>	<i>Value</i>
Wavelength (Å)	0.97918
Space group	P2 ₁
Cell Parameters	a = 37.59, b = 77.55, c = 54.78, β= 99.73
Resolution (Å)	30 - 2.75 (2.85 - 2.75)
No. of observations	31885
No. of unique reflections	8227
Completeness (%)	98.6 (97.9)
R _{sym} ^a	0.134 (0.485)
I/σ(I)	10.3 (2.0)
Refinement statistics	
Resolution range	30-2.75 (2.85 - 2.75 Å)
R factor, %	22.33 (34.67)
R _{free} , %	28.76 (39.32)
Wilson B factor (Å ²)	42.1
Molecules / Asym unit	2
Residues	2 X 149
<u>Atoms</u>	
Protein	2346
Solvent	207
Cofactor (FAD)	106
Mean B-values (Å ²)	
Overall	41.7 Å ²
Main chain	40.8 Å ²
Side chain	42.7 Å ²
Solvent	33.0 Å ²
Rmsd from ideal geometry	
Bonds	0.017 Å
Angles	2.14°
Ramachandran plot, %	
Most favored	83.6
Additionally allowed	15.6
Generously allowed	0.8
Disallowed	0.0
Missing residues	None

$$^a R_{\text{sym}} = \frac{\sum_j |I_j - \langle I \rangle|}{\sum_j I_j}$$

Reference

1. J. S. Lamb, B. D. Zoltowski, S. A. Pabit, L. Li, B. R. Crane, L. Pollack, Illuminating solution responses of a LOV domain protein with photocoupled small-angle x-ray scattering. *J. Mol. Biol.* **393**, 909–919 (2009).